

## Enhancement of the light output of GaN-based ultraviolet light-emitting diodes by a one-dimensional nanopatterning process

Hyun-Gi Hong, Seok-Soon Kim, Dong-Yu Kim, and Takhee Lee

*Department of Materials Science and Engineering, Gwangju Institute of Science and Technology, Gwangju 500-712, Korea*

June-O. Song

*School of Electric and Computer Engineering, Georgia Institute of Technology, Atlanta, Georgia 30332-0250*

J. H. Cho, C. Sone, and Y. Park

*Photonics Program Team, Samsung Advanced Institute of Technology, Suwon 440-600, Korea*

Tae-Yeon Seong<sup>a)</sup>

*Division of Materials Science and Engineering, Korea University, Seoul 136-713, Korea*

(Received 13 October 2005; accepted 9 January 2006; published online 8 March 2006)

We have demonstrated the enhancement of the output power of ultraviolet GaN-based light-emitting diodes (LEDs) by using one-dimensionally nanopatterned Cu-doped indium oxide(CIO)/indium tin oxide (ITO) *p*-type contact layers. The one-dimensional (1D) nanopatterns (250 nm in width and 100 nm in depth) are defined using a TiO<sub>2</sub> 1D nanomask fabricated by means of a surface relief grating technique. When fabricated with the nanopatterned *p*-contact layers, the output power of LEDs is improved by 40 and 63% at 20 mA as compared to those fabricated with the unpatterned CIO/ITO and conventional Ni/Au contacts, respectively. © 2006 American Institute of Physics. [DOI: 10.1063/1.2174842]

GaN-related semiconductor materials are of great technological importance for the fabrication of optoelectronic devices.<sup>1,2</sup> In particular, an increase of light extraction efficiency in GaN-based light emitting diodes (LEDs) is a crucial issue.<sup>3</sup> It was reported that internal quantum efficiency reaches over 80% due to the development of growth techniques.<sup>3</sup> However, external quantum efficiency is still very low as compared with internal quantum efficiency. One major reason is related to high refractive index (2.1–2.5 at 405 nm) of GaN-related materials and indium tin oxide (ITO) top contact layers, resulting in the escape cone with a small angle for the emitted light, and so causing most of the light to experience total internal reflection. Thus, to enhance the light extraction efficiency, several methods, such as laser lift-off, GaN surface roughening, and contact layer patterning, were introduced.<sup>4–9</sup> In particular, a contact-layer patterning technique was found to be efficient in enhancing light extraction by inducing the photonic crystal effect. For example, Pan *et al.*<sup>8</sup> showed that the microsized patterning of ITO top transparent electrodes results in an increase of output power (at 20 mA) up to 16% without the degradation of the electrical properties of the electrodes. Wierer *et al.*<sup>9</sup> reported that the introduction of photonic crystal structures leads to the enhancement of the radiance of InGaN/GaN LEDs. For commercial application, however, a low-cost and reproducible method is desirable. In this work, we used a surface relief grating (SRG) technique to define one-dimensional (1D) nanopatterns on transparent *p*-type electrode layers for ultraviolet (UV) (385 nm) LEDs.<sup>10</sup> The SRG method is an anisotropic and cheap process, where expensive equipment, such as electron-beam (e-beam) lithography, is

not required. A Cu-doped indium oxide (CIO)(3 nm)/ITO(400 nm) scheme was used as a top *p*-contact layer because of its high transmittance of ~90% at 385 nm and good ohmic behaviors.<sup>11</sup> It is shown that the 1D nanopatterning of the CIO/ITO electrodes is very effective in enhancing the output power of LEDs.

GaN-based UV (385 nm) LED structures were fabricated using metalorganic chemical vapor deposition. The LED structure was comprised of a GaN buffer layer, *n*-GaIn, an InGaIn/GaN multiquantum-well active layer, and *p*-GaIn. Dry etching was used to create 300 μm × 300 μm mesa-structure of LEDs. The CIO(3 nm)/ITO(400 nm) *p*-contact layers were deposited on *p*-GaIn by e-beam evaporation. After lift off, the LEDs were annealed at 630 °C for 1 min in air. After fabricating full LED structures, a 1D nanopatterning process proceeded. The details of the nanopatterning process will be published elsewhere.<sup>10</sup> Azobenzene-functionalized polymer film poly (disperse orange 3) (500 nm thick) was deposited on the LEDs by spin coating followed by drying. The SRGs were fabricated on the polymer film using an interference pattern of an Ar<sup>+</sup>-laser beam at 488 nm. To fabricate a 1D TiO<sub>2</sub> nanomask, a drop of Ti isopropoxide in 2-propanol containing HCl was placed on the SRGs, and then immediately spun at room temperature. Spin-coated material was heat treated for 12 h through the several steps (room temperature → 100 °C → 400 °C → 425 °C) to remove the polymer template and to avoid the cracking of the 1D TiO<sub>2</sub> mask. The resultant ITO with the 1D TiO<sub>2</sub> mask was selectively etched using inductively coupled plasma etching to prevent the formation of ITO residues and excess sidewall etching occurring as a result of a wet etching process. Finally, the 1D TiO<sub>2</sub> nanomask was selectively removed by reactive ion etching in a CF<sub>4</sub> plasma. Furthermore, for comparison, LEDs with 630 °C-annealed

<sup>a)</sup> Author to whom correspondence should be addressed; electronic mail: tyseong@korea.ac.kr

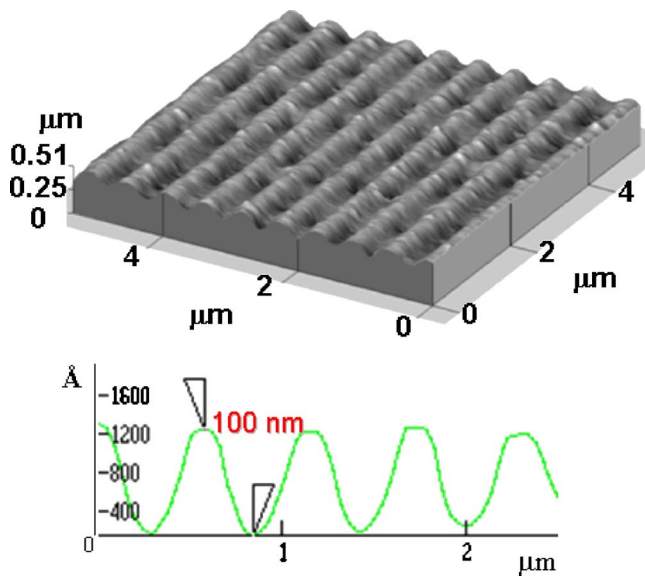


FIG. 1. (Color online) AFM images of the 1D nanopatterned ITO and its depth profile. The width, depth, and spacing of patterns are 250, 100, and 250 nm, respectively.

unpatterned CIO/ITO layers and 530 °C-annealed Ni(5 nm)/Au(5 nm) layers were also fabricated. The morphology of 1D nanopatterned LEDs was examined by scanning electron microscopy (SEM) (Hitachi, S-4700) and atomic force microscopy (AFM) (PSI, Auto probe CP). Current-voltage ( $I$ - $V$ ) characteristics of LEDs were investigated using a parameter analyzer (HP4155A). Output power and electroluminescence (EL) were also characterized.

Figure 1 shows an AFM image of an 1D nanopatterned ITO surface and its depth profile. An unpatterned ITO layer (not shown) exhibited a very smooth surface with a root-mean-square (rms) roughness of 3.1 nm. In addition, it showed a sheet resistance of 43.28  $\Omega$ /sq. and transmittance of 90% at 385 nm. However, after etching, an array of well-defined 1D nanopatterns is formed on the whole ITO surface. The width and depth of the 1D nanopatterns are measured to 250 and 100 nm, respectively. The spacing between individual patterns was measured to be 250 nm.

Figure 2 shows SEM images of the 1D nanopatterned LED structure. As shown in Fig. 2(a), a top-view image exhibits that LEDs with the nanopatterned CIO/ITO  $p$ -contact layers are successfully fabricated. Figures 2(b) and 2(c) show that the CIO/ITO  $p$ -contact layers are one dimensionally patterned, which is in agreement with the AFM results. Furthermore, the GaN surface was also etched slightly because the etching selectivity of ITO and GaN is not perfect. However, this may not degrade the electrical properties of the patterned LEDs, as will be described later.

Figure 3(a) shows the  $I$ - $V$  characteristics of the LEDs with the CIO/ITO and conventional Ni/Au  $p$ -contact layers before and after nanopatterning. Both the nanopatterned and unpatterned CIO/ITO LEDs show fairly similar  $I$ - $V$  characteristics, both better than that of the Ni/Au LEDs. The patterned CIO/ITO LEDs give a forward voltage of 3.35 V at 20 mA and series resistance of 18.54  $\Omega$ , whereas the unpatterned CIO/ITO and Ni/Au LEDs produce 3.36 and 3.45 V at 20 mA, and a series resistance of 19.97 and 24.14  $\Omega$ , respectively. EL was measured as a function of the wavelength at 20 mA. Figure 3(b) shows EL data of the nanopatterned and unpatterned LEDs with different  $p$ -contact layers. It is

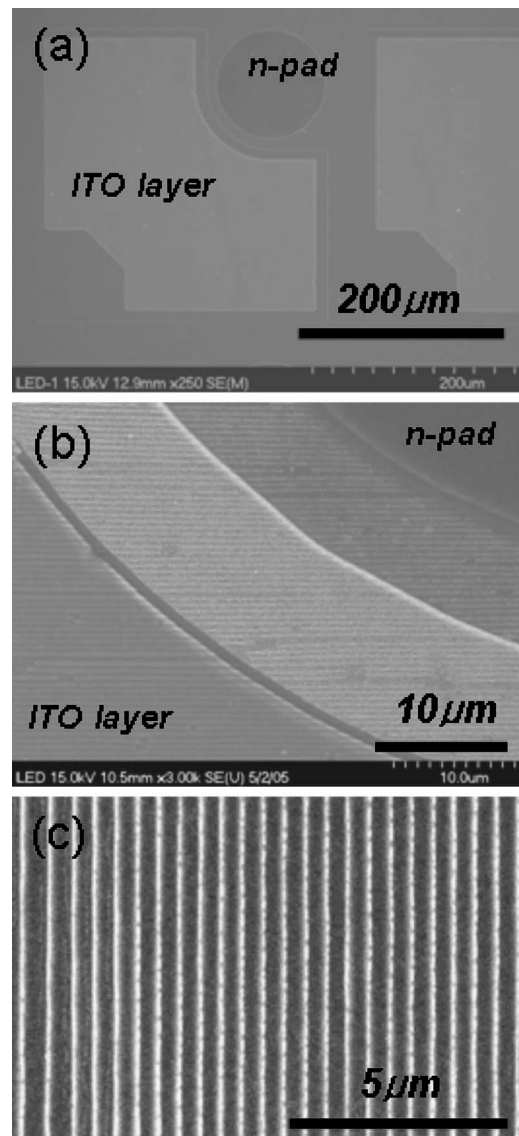


FIG. 2. (a) A top-view SEM image of the 1D nanopatterned LED structure. (b) and (c) Enlarged images.

noted that irrespective of the nanopatterning process, the EL peak position (385 nm) of the LEDs remains unchanged and the nanopatterned CIO/ITO LEDs produce the strongest EL among the three samples.

Figure 4 shows the output-current ( $L$ - $I$ ) characteristics of the nanopatterned CIO/ITO LEDs, the unpatterned CIO/ITO LEDs, and the conventional Ni/Au LEDs as a function of the forward drive current. It is evident that the light output power of the LEDs with the nanopatterned CIO/ITO contact layers is much higher than those of the unpatterned CIO/ITO and Ni/Au LEDs across the whole current range. For example, for the LED with the nanopatterned CIO/ITO contact layer, its output power at 20 mA was improved by 40 and 63% as compared with those of the LEDs with the unpatterned CIO/ITO and Ni/Au  $p$ -contact layers, respectively. This shows that the nanopatterning of the electrode surface is very effective in improving the performance of the LEDs without the degradation of their electrical properties.

The nanopatterning process resulted in an insignificant change of the electrical performance of LEDs, although the turn-on voltage increased slightly (by 0.05 V) and the series resistance decreased slightly (by 1.43  $\Omega$ ). The slight increase

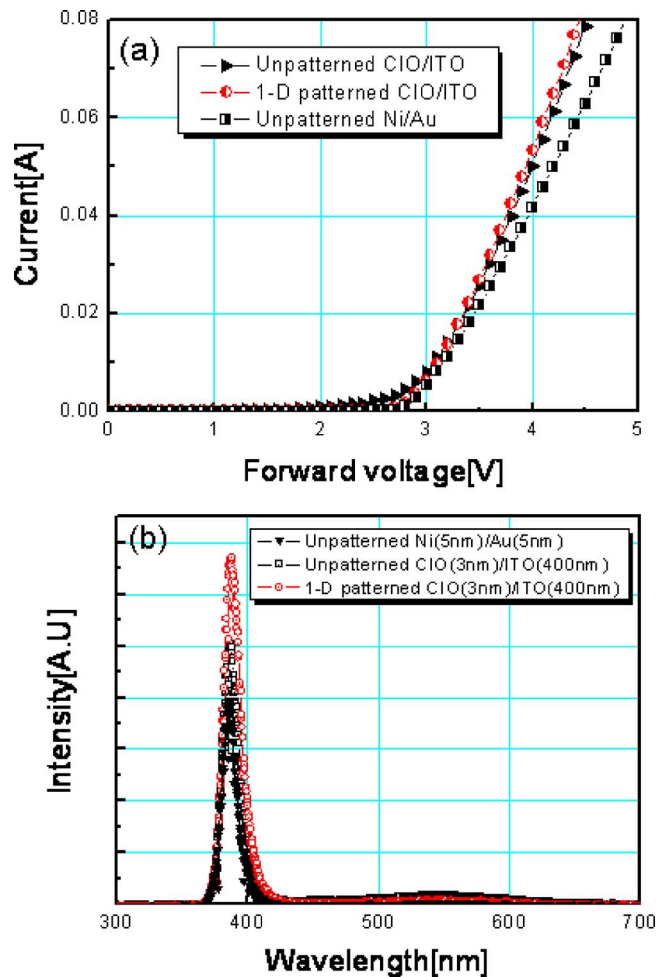


FIG. 3. (Color online) (a) The  $I$ - $V$  characteristics and (b) EL data of LEDs made with the 1D nanopatterned CIO(3 nm)/ITO(400 nm), unpatterned CIO(3 nm)/ITO(400 nm), and conventional Ni(5 nm)/Au(5 nm) contacts.

of the turn-on voltage may be associated with a reduction of the surface area of the electrode, which is in contact with a probe tip for the power supply. The decreased series resistance after patterning could be attributed to a decrease of the sheet resistance of ITO (changing from 43.28 to 34.14  $\Omega$ /sq). During the patterning process, the ITO films experience heat treatment (from 100 to 425  $^{\circ}$ C), which gives rise to a reduction of the sheet resistance. In this

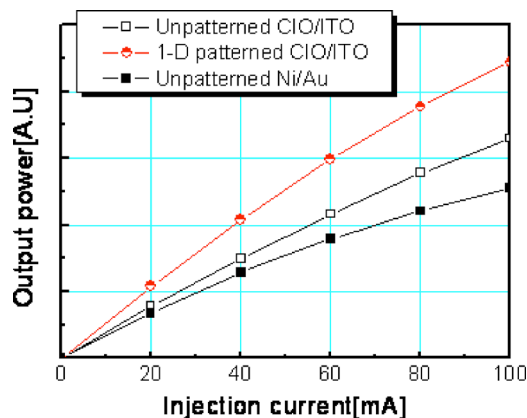


FIG. 4. (Color online) The  $L$ - $I$  characteristics of LEDs fabricated with the 1D nanopatterned CIO/ITO, unpatterned CIO/ITO, and conventional Ni/Au contacts as a function of the forward drive current.

work, the output power of the nanopatterned samples was improved by 40% compared with that of the unpatterned sample. The improvement can be attributed to the formation of one dimensionally arranged nanopatterns, as shown in the AFM and SEM results (Figs. 1 and 2). According to the Snell's law,<sup>12</sup> the critical angle ( $\theta_{\text{crit}}$ ) of total internal reflection is given by  $\theta_{\text{crit}} = \sin^{-1}(n_1/n_2)$ , where  $n_1$  and  $n_2$  are refractive indexes of two different media, respectively. Using the optical parameters of GaN, ITO, and air, e.g.,  $n_{\text{GaN}}=2.6$ ,  $n_{\text{ITO}}=2.15$ , and  $n_{\text{air}}=1.0$  at a wavelength of 385 nm, the critical angles ( $\theta_{\text{crit}}$ ) were calculated to be 55.8 $^{\circ}$  and 27.7 $^{\circ}$  with respect to the direction perpendicular to the surface for the GaN/ITO and ITO/air interfaces, respectively. For simplicity, we ignored  $n_{\text{CIO}}$  of a CIO layer between the ITO and GaN layers, since the CIO layer was broken into nanodots (5–45 nm in size). For the unpatterned sample, emitted light having incident angles smaller than  $\theta_{\text{GaN/ITO}}$  of 55.8 $^{\circ}$  can escape from the ITO/GaN interface and the escaped light inside the angle ( $\theta_{\text{ITO/air}}$  of 27.7 $^{\circ}$ ) can be finally extracted. However, the light outside the escape cone ( $\theta_{\text{ITO/air}}$  of 27.7 $^{\circ}$ ) is reflected and so trapped inside the GaN region. For the 1D nanopatterned sample, the patterning resulted in the formation of sidewalls as well as the reduction of unpatterned flat regions. This can cause some of internally reflected light outside of the escape cone ( $\theta_{\text{ITO/air}}$  of 27.7 $^{\circ}$ ) to escape through the sidewall ITO/air interfaces, resulting in additional light extraction, as demonstrated by the light output power of LEDs fabricated with these ITO layers before and after 1D ITO nanopatterning (Fig. 4).

In conclusion, we have introduced the 1D nanopatterned electrodes to fabricate high-performance UV LEDs. It was shown that the use of the 1D nanopatterned structures results in the enhancement of the light output of LEDs by 40% as compared with unpatterned LEDs, and by 63% compared to the conventional Ni/Au LEDs. The result implies that the 1D nanopatterning technique could be a technologically important process for the fabrication of high-brightness UV LEDs for solid-state lighting.

- <sup>1</sup>S. Nakamura, T. Mukai, and M. Senoh, Appl. Phys. Lett. **64**, 1687 (1994).
- <sup>2</sup>D. A. Steigerwald, J. C. Bhat, D. Collins, R. M. Fletcher, M. O. Holcomb, M. J. Ludowise, P. S. Martin, and S. L. Rudaz, IEEE J. Sel. Top. Quantum Electron. **8**, 310 (2002).
- <sup>3</sup>T. Nishida, H. Saito, and N. Kobayashi, Appl. Phys. Lett. **79**, 711 (2001).
- <sup>4</sup>J. J. Wierer, D. A. Steigerwald, M. R. Krames, J. J. O'Shea, M. J. Ludowise, G. Christenson, Y.-C. Shen, C. Lowery, P. S. Martin, S. Subramanya, W. Gotz, N. F. Gardner, R. S. Kern, and S. A. Stockman, Appl. Phys. Lett. **78**, 3379 (2001).
- <sup>5</sup>J.-O. Song, J. S. Kwak, and T.-Y. Seong, Appl. Phys. Lett. **86**, 062103 (2005).
- <sup>6</sup>D. W. Kim, H. Y. Lee, M. C. Yoo, and G. Y. Yeom, Appl. Phys. Lett. **86**, 052108 (2005).
- <sup>7</sup>T. Fujii, Y. Gao, R. Sharma, E. L. Hu, S. P. Denbaars, and S. Nakamura, Appl. Phys. Lett. **84**, 855 (2004).
- <sup>8</sup>S.-M. Pan, R.-C. Tu, Y.-M. Fan, R.-C. Yeh, and J.-T. Hsu, IEEE Photonics Technol. Lett. **15**, 649 (2003).
- <sup>9</sup>J. J. Wierer, M. R. Krames, J. E. Epler, N. F. Gardner, M. G. Craford, J. R. Wendt, J. A. Simmons, and M. M. Sigalas, Appl. Phys. Lett. **84**, 3885 (2004).
- <sup>10</sup>S.-S. Kim, C. Chun, J.-C. Hong, and D.-Y. Kim, J. Mater. Chem. (to be published).
- <sup>11</sup>J.-O. Song, J. S. Kwak, Y. Park, and T.-Y. Seong, Appl. Phys. Lett. **86**, 213505 (2005).
- <sup>12</sup>T. Nakamura, N. Tsutsumi, N. Juni, and H. Fujii, J. Appl. Phys. **97**, 054505 (2005).